Available online at www.sciencedirect.com

ScienceDirect

Procedia CIRP 65 (2017) 273 – 278

www.elsevier.com/locate/procedia

3rd CIRP Conference on BioManufacturing

Optimizing the architecture of a dynamic spinal implant for customized mechanical behavior

Yann Ledoux [a], Antonio Ramos [b], Michel Mesnard [a, *]

[a] *Université de Bordeaux, Institut de Mécanique et d'Ingénierie, CNRS UMR 5295, 33405 Talence, France*
[b] *University of Aveiro, Department of Mechanical Engineering, 3810-193 Aveiro, Portugal*

* Corresponding author. *Tel.:* +33-607-688-092. *E-mail address:* michel.mesnard@u-bordeaux.fr

Abstract

Non-fusion technology in spine surgery reduces surgical morbidity and degeneration of the adjacent levels by the insertion of dynamic spinal implants. Despite these advantages, a dynamic spinal implant (DSI) generates complications which require clinical follow-up, the continuous development of constructive solutions and structured optimization of the implant architecture using current mechanical design methods.
This study structures this optimization process of a DSI concept by incorporating the mechanical behavior of the device, design variables and functional requirements into a global design model. The geometric (descriptive anatomy) and mechanical (materials, components, etc.) characteristics are obtained from a literature review. By combining these parameters, variables and requirements, appropriate values can be determined. The resulting mathematical model is then used to design and implement a device that is suitably adapted in movements and stiffness. The model assumes linear or non-linear behavior.
We describe the optimization of the design variables to ensure the correct functioning of the mechanism when adapted to the patient. The optimization purpose is to determine the architecture of the implant, the choice of materials and the geometric parameters of implantation. An optimized implant model corresponding to specific degrees of degeneration in the intervertebral joint can then be envisaged.

Peer-review under responsibility of the scientific committee of the 3rd CIRP Conference on BioManufacturing 2017

Keywords: Dynamic implant; Design; Mechanical Model; Optimization.

1. Introduction

More than 5% of the world's population suffers acute back pain, especially as a result of degenerative pathologies of intervertebral discs. This degeneration leads to deterioration in the disc properties (loss of shock absorption, collapse, disc herniation, etc.).

The lumbar spinal segments are highly stressed and particularly badly affected during movement and when carrying loads. Disabling pain (lumbago) is usually accompanied by nerve pain (sciatica, cruralgia) which can generate a risk of paralysis.

The initial treatment of disc degeneration is to apply conservation options (drugs, rehabilitation, etc.); 5% to 10% of patients find no relief. Implant surgery is then the second treatment option to improve quality of life.

The fusion technique is often used in spine surgery and is the benchmark treatment. Posterior instrumentation (pedicle screws and rods) results in the complete and definitive suppression of mobility in the operated segment. Although the clinical results may be satisfactory, this technique can have some highly negative consequences: accelerated degeneration of the adjacent vertebral levels, screw loosening, etc. [1].

As a result, more recently, "non-fusion" systems have gradually been developed. The aim of these dynamic spinal implants (DSI) is to limit the evolution of the pathology, to preserve partial mobility and to reduce intradiscal pressure. Kaner proposes a classification of these DSIs into two groups: anterior devices and posterior devices [2].

Anterior devices include total disc prostheses and nucleus pulposus prostheses (core) where only the central part is replaced. Posterior devices [3] cover three types of systems:

Peer-review under responsibility of the scientific committee of the 3rd CIRP Conference on BioManufacturing 2017
doi:10.1016/j.procir.2017.04.056

interspinous systems, systems that replace the facet joints, and pedicle systems [4]. Posterior devices with pedicle screws are able to preserve the integrity of the disc and the facets.

The lumbar segment studied here is implanted with an innovative posterior DSI (Fig. 1) consisting of two rigid metal elements (piston rod and fixed rod made of titanium) and deformable polymer elements inserted in the cylinder. The two rods are fixed to the pedicles of the lumbar vertebrae using titanium pedicle screws. The piston rod is connected to the upper vertebra (denoted n) and the fixed rod to the lower vertebra (denoted n+1). An assembly consisting of two DSIs and four pedicle screws is needed for one joint segment.

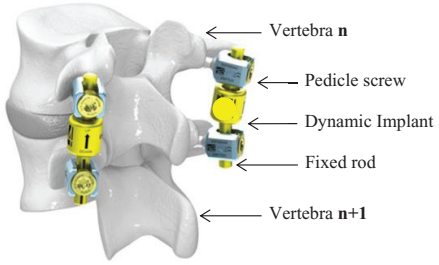

Fig. 1. Innovative concept for a dynamic spinal implant (articular segment **n/n+1**).

The main function of the assembly is to ensure the transfer of loads and to stabilize the lumbar segment during the three types of anatomical movement: flexion-extension, lateral inflexion and axial rotation. It must therefore allow mobility but also limit the range of relative movements. During extension movements by the patient the implants undergo compression. During flexion movements, they undergo traction.

Several solutions have been studied; this innovative concept has been validated by mechanical tests (quasi-static traction-compression, fatigue and aging accelerated by DMA), a key step in the design process devised for these medical devices [5] [6].

There is considerable intervariability in the range of displacement and the degree of the pathology in a significant sample of patients. The aim can never be to control these variations but to analyze them in order to design then optimize devices that perform their functions by incorporating natural fluctuations into these pathological situations. To do this, the optimization study is based on a structuring system (see section 3), involving Observation, Interpretation and Aggregation steps (OIA) which includes design constraints and the intended goals for the DSI.

A parsimonious model was developed, based on the geometry and mechanical characteristics of the assembly. The mechanical construction data for this model are derived from a previous experimental and bibliographic study, evaluating the displacements, the actions transmitted and their load distributions [7]. Thus the model that was constructed included mechanical behavior and these functional requirements. Sets of solutions were tested according to levels of degeneration (pathology); finally, a compromise was sought to meet the needs of a targeted sample of patients by developing the DSI.

2. Developing the mathematical model

The literature reveals essentially two types of modeling of the lumbar spine. The models most often produced are based on finite element (FE) methods. They study the local behavior of the vertebral column and include the non-linear mechanical behavior of vertebral segments (intervertebral disc), the influence of muscles and ligaments, etc. [8]. This detailed modeling is adapted to assess the state of stress of the elements of the vertebral segments after implantation.

The aim is to develop a predictive mechanical model during the design phase of a DSI; detailed FE models give access to stresses in all elements of the vertebra and the disc. This information is essential from a clinical point of view and during the validation phase of the technological solutions. In this study, we intend only to differentiate the positions of the constituent elements of the solutions and their intrinsic stiffness so as to adapt them as well as possible to the different degrees of disc degeneration. As a result, a simplified dimensioning tool is needed in this upstream solution search phase [9]. Different models can then be selected. In an earlier study, we used a model consisting of rigid bodies subjected to forces in mechanical equilibrium [10]. The main advantage of this model is that it is possible to assess the solution behavior with a very short calculation time (resolution of an analytical model); however, the equation system is associated with a single specific architecture of the solution. In order to put in place a tool that can be more generally applied, we develop a FE model consisting of beam elements and springs, using Matlab. The resolution times remain comparable but this model can evolve and one may envisage other architectures.

In this study, we model the mechanical behavior of a segment of the lumbar spine, taking into account the natural and postoperative asymmetries with respect to the sagittal plane (where the range of displacements is greatest during flexion or extension movements). The model is formulated based on relationships that represent the equilibrium of a mechanical system (Newton's first law). It can describe the natural behavior of the vertebral segment and its behavior after implantation of the DSI. The modeling process is described in the following paragraphs.

2.1. Disc degeneration and load distribution

According to the literature, the gradual degeneration of the disc produces a change in the load-bearing areas between the vertebrae. According to [10], when the disc is functioning in a standard way, the vertical load is mainly supported by the contact between the vertebra and the disc surface and is distributed between the anterior and posterior halves of the vertebra body. A fraction of the vertical load is taken up by the neural arch (around 8%). As a result of degeneration, this distribution changes considerably. Depending on the degree of degeneration, the load taken up by the neural arch can change from 8% of the vertical load to 63% in extreme cases. This variation is described in Table 1 based on cadaveric measurements [7] [10]. According to these measurements, in the lumbar region, the vertical load between vertebrae is 2kN.

This load magnitude was confirmed by our previous study [10] in the upright position, for standard conditions, without additional external loads. It takes into account the weight of the body upper part and the action of the tendons and muscles.

Table 1. Load distributions according to [10]; Mean values ± SD for each grade of disc degeneration (s is the number of specimens).

Upright posture			
Deterioration	Ant. vertebra	Post. vertebra	Neural arch
Grade 1 (s=6)	44 ± 11	48 ± 5	8 ± 8
Grade 2 (s=11)	33 ± 16	48 ± 12	19 ± 14
Grade 3 (s=28)	19 ± 13	47 ± 14	34 ± 17
Grade 4 (s=19)	11 ± 8	26 ± 16	63 ± 22

It is no easy task to model the estimated mechanical behavior of the lumbar region. Referring to works which are based on plastic elasto-visco models of the components of the lumbar region (disc, vertebra, etc.), in this study, we intend only to estimate the effect on the overall functioning of the lumbar region of adding a DSI. Thus we model the natural lumbar region with elastic behavior (assuming a linear behavior of the displacement in relation to the load), whose characteristics are given in Figure 1. These characteristics are derived from studies by [5], [9] and [10] for the disc and vertebra behavior respectively.

In order to include stiffness values in a mechanical model, we must introduce the characteristic dimensions of the elements. To do this, we produced a synthesis of data from the literature studying the main morphological characteristics of the lumbar region (from L1 to L5). The data came mainly from [10]. Figure 2 lists the main parameters and the values selected. Based on the dimensions of every component, an equivalent stiffness can be computed for the lumbar zone (later called K_{eq}) equal to 872N.mm^{-1}.

Characteristics (N.mm^{-1})	
K_{vert}	3000
K_{disc}	926

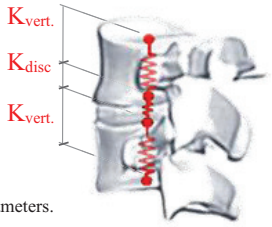

Fig. 2. Mechanical parameters.

As the degeneration of the disc (see 2.1) leads to a gradual transfer of the center of pressure (denoted O) of the 2kN vertical load (denoted F) along the line AE (Fig. 3), we note that the distance BO varies from 3.4mm to 25.7mm for the most serious degeneration grade.

Dimension (mm)		
AB	AC	AE
22.4	44.8	76.5

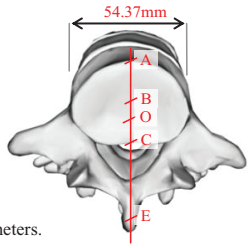

Fig. 3. Geometrical parameters.

For grade 4, it should be stressed that the centre of pressure is located at the exterior of the contact surface between the vertebra and the disc as described in Table 1.

Table 2. Distance BO according to the degeneration grade.

Deterioration grade	Load sharing along segment (%)			Distance (mm)
	AB	BC	CE	BO
1	44	48	8	3.4
2	33	48	19	9.3
3	19	47	34	16.5
4	11	26	63	25.7

2.2. Modeling the mechanical behavior of the DSI

The main advantage of using the DSI is to rebalance this transfer of load. To quantify this, a mechanical parametric model needs to be developed of the entire lumbar region and the DSI (Fig. 4).

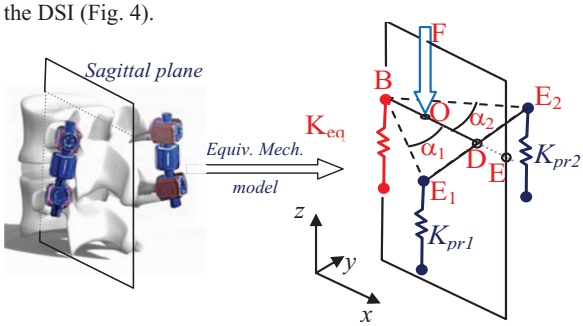

Fig. 4. Definition of the equivalent mechanical model.

The mechanical model we developed is based on a FE assembly using 3D elements of the Bernoulli Beam type (for sections BO, OD, E_1D and E_2D). Local stiffnesses were added at points B, E_1 and E_2 to introduce the contribution of the vertebrae (K_{eq}) and the elements of the DSI, K_{pr1} at E_1 and K_{pr2} at E_2 respectively. The external loading was applied at point O (F_z = -2kN). With this configuration, 3D beam elements with 6 degrees of freedom per node must be used. Displacement boundary conditions were imposed at point B ($u_x = u_y = 0$), point O ($u_y = 0$) and point D ($u_y = 0$). Properties were chosen for sections BO, OD, E_1D and E_2D a profile with a circular cross-section (radius 0.01m) where E = 210000MPa (Young's modulus) and $\nu = 0.3$ (Poisson's ratio). It could be noticed that only the displacements of point B, E_1 and E_2 were relevant in this modeling; the characteristics of beams have been selected without any consideration of the natural element and they are only used to transfer the vertical load applied in point O to the other points. By resolving the matrix system constructed from the assembly of elementary stiffness matrices and introducing boundary conditions, it was possible to identify the depressions along axis z for points B, E_1 and E_2 for a parameterization of the dimensions (BO, OD, E_1D and E_2D) and angles (α_1 and α_2), by resolving the system of equations 1. To determine the angle variation of plane B, E_1, E_2, we calculate the normal of this plane from equation 2 and then to deduce the characteristic angles β (between this normal and axis z in plane x, z) and θ (between this normal and axis z in plane y, z).

$$\mathbf{f} = K\,\mathbf{u} \quad (1)$$

with K, the stiffness matrix of the structure, **f,** the load vector applied to the system and **u**, the displacement vector of every node.

$$\mathbf{n} = \mathbf{BE_1} \times \mathbf{BE_2} \quad (2)$$

with **n**, the normal of the plane defined by points B, E_1 and E_2.

From the normal, vector **n**, the different angle value defined in equations 3 and 4 could be deduced.

$$\theta = \text{atan}(\mathbf{n.y} / \mathbf{n.z}) \quad (3)$$
$$\beta = \text{atan}(\mathbf{n.x} / \mathbf{n.z}) \quad (4)$$

With the mechanical model we developed, we were able to determine the influence of the addition of the DSI to the assembly of vertebrae as a function of angles α_1, α_2, screw length through distances BE_1 and BE_2 and degree of degeneration of the disc (from 2 to 4) parameterizing the position of the center of pressure O. We observed an angle deviation both in the sagittal plane (β) and the frontal plane (θ), linked with the independent parameterizing of the angles and screw lengths.

3. Structuring the design optimization problem

As the aim of the study is to optimize the behavior of the joint segment for the different degrees of degeneration associated with the pathology, the DSI should restore kinematics and load transfer on the joint, whatever the patient.

This study structures the problem using the "Observation - Interpretation - Aggregation" (OIA) formulation suggested by the works of Collignan [11] and Quirante [12]. Three models were produced: **i.** the observation model includes the mathematical model (see 2.2); **ii.** then, the interpretation model defines an interpretation function to identify solutions of interest; **iii.** the aggregation model translates all the objectives into a single objective to be optimized (Fig. 5). This approach has been validated when systems were optimized, mainly by Quirante [13] and Sebastian [14].

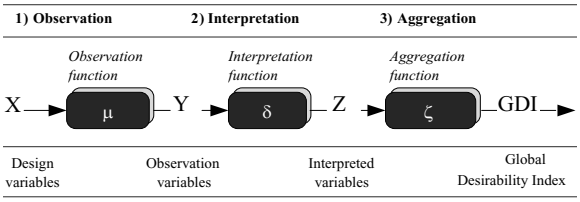

Fig. 5. Structuring of the design problem through the observation, interpretation and aggregation model [10].

Thus a single function translates the designer's preference (iii) by defining weights associated to the design constraints. The solution can then be filtered by aggregation, as described in studies by Harrington [15]. Details of the design model are shown in Figure 5. In the next two paragraphs (3.1 and 3.2) the variables are described and the three models are presented.

3.1. Variables, functional requirements, observation model

Designing the DSI involves determining the parameter values of the different models developed in part 2 of this study. The implantation parameters of the screws can be identified mainly by: angles α_1 and α_2, screw lengths (BE_1 and BE_2), compressive stiffness of the DSI (K_{pr1} and K_{pr2}). Table 3 lists the variations envisaged for each of the six design parameters.

Table 3. Name and range of the design parameters.

	Design parameters					
	α_1 (°)	α_2 (°)	BE_1 (mm)	BE_2 (mm)	K_{pr1} (N.mm^{-1})	K_{pr2} (N.mm^{-1})
Range	[10;30]	[10;30]	[65;100]	[65;100]	[200;1500]	[200;1500]

3.2. Observation, interpretation, aggregation functions

The observation model, presented in Figure 5 and developed in Section 2, makes it possible to link the six design variables to different quantities in order to judge the relevance of these values of design variables (called design criteria). From a functional point of view, there are three criteria with which to judge the relevance of a solution. Angle Δβ ensures that the disc remains both in contact and load-bearing despite the use of the DSI. If this is not the case, there is a considerable risk that osteoporosis may develop. In addition, angle Δθ is used to check that the load distribution remains centered on the axis of the vertebral column despite the dispersions associated with the implantation phase. For these two angle parameters, the variation should be between ±5°. In the event of design problems, we suggest limiting the variation in the height of points ΔE_1 and ΔE_2 to [-2; 1].

From these design requirements, the acceptability of a design solution can be defined as its ability to satisfy every design criterion. In our case, these criteria are expressed in different units (mm and d°), making a direct comparison between them difficult. The interpretation of the design criteria consists in bringing criteria to a scale of comparison by qualifying their degree of satisfaction. In this way, desirability functions are a class of value functions which turn criteria into a satisfaction level ranging from 0 (undesirable) to 1 (full satisfaction level). The interpretation functions correspond to those of Harrington, shown in Figure 6 [15].

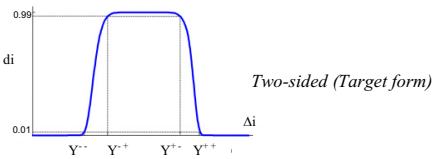

Fig. 6. Shape of Harrington's interpretation functions.

According to the constraint types, we use a two-sided function since the objective is to target particular values. The interpretation functions are customized by the bound Y^{--}, Y^{-+}, Y^{+-} and Y^{++}. Their values are given in Table 4.

Table 4. Desirability boundary definitions.

	ΔE_1 and ΔE_2 (mm)		Δβ and Δθ (°)	
	$\{ Y^{--}, Y^{-+} \}$	$\{ Y^{+-}, Y^{++} \}$	$\{ Y^{--}, Y^{-+} \}$	$\{ Y^{+-}, Y^{++} \}$
Grade 2 to 4	{-2, -1.9}	{0.9, 1}	{-1.5, -1}	{1, 1.5}

From the different desirability values (from $d\Delta E_1$, $d\Delta E_2$, dΔβ, dΔθ we propose to compute the Global Desirability Index

(GDI) for the product of every desirability value. Different aggregation strategies could be used to compute the GDI. In our case, a solution should respect every design criterion and compensatory strategy is not suitable for the design of the DSI. The GDI is computed according to equation 5.

$$GDI = (d\Delta E_1 \cdot d\Delta E_2 \cdot d\Delta\beta \cdot d\Delta\theta) \quad (5)$$

4. Solving process and results

4.1. Observation, interpretation, aggregation functions

The main advantage of using a simplified model lies in the fact that the time required to find a solution is shorter. This allows for a combinatorial exploration of the design space. The scope of each design variable is defined in Table 4. For each one, a unit increment (i.e. 1° or 1mm) was tested. For stiffness values K_{pr1} and K_{pr2}, an increment of 100N.mm^{-1} was used. We first assume a problem where the implantation parameters and the implant stiffnesses are symmetrical (i.e. $BE_1 = BE_2$; $\alpha_1 = \alpha_2$ and $K_{pr1} = K_{pr2}$). Using this hypothesis, the solution space can be limited to a 3D space. The aim is then to determine the combinations of design variables that maximise the GDI for each grade.

Graphs form a to d in Figure 7 show the different combinations of design variables where the GDI value is greater than 0.2. Note that, depending on the degree of degeneration, the design variable combinations of relevant solutions are not identical. They range from grade 2, with a small area of solutions and about 1000 combinations of variables (Fig. 7.a), to 7000 solutions for grade 3 (Fig. 7.b), then 9800 solutions for grade 4 (Fig. 7.c). This justifies the use of this type of device for high degrees of degeneration.

We also note that for grade 2 the K_{pr1} and K_{pr2} values are low, at 200N.mm^{-1} whatever the values of α and BE_i (corresponding to values of BE_1 and BE_2). For this configuration of stiffnesses the GDI is close to one, meaning that the design constraints are respected. Concerning grade 3, the solution areas with high GDI values are to be found where the K_{pr1} and K_{pr2} values are below 600N.mm^{-1} and, as was the case for grade 2, the other two variables have little influence on the GDI. And finally, for the last grade, in contrast to the other two, we note that the solution area is limited for the lowest stiffness values.

In order to design a DSI that is compatible with all the different degrees of degeneration, we looked for the intersection of all the solutions for these 3 grades. The value of the resulting GDI was the cube root of the product of the GDIs obtained for each grade (Fig. 7.d). One can see that the intersection greatly limits the number of solutions and we obtained only 369 different solutions. Thus, for the envisaged load, it is apparent that the low levels of DSI stiffness seem better adapted to all the grades of degeneration, with lengths BE_i between 90 and 100mm and angles of implantation varying between 10 and 30°.

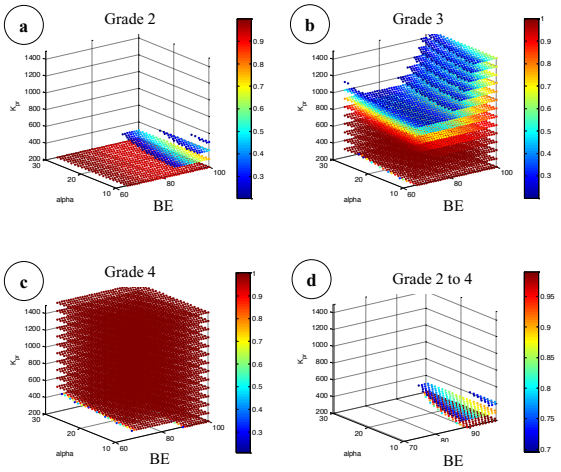

Fig. 7. Location of relevant solutions (ie. with GDI over than 0.2)

4.2. Robustness of solutions

When the device is being implanted, the surgeon must cope with various problems in order to guarantee the ideal implantation parameters. This is mainly due to morphological intervariability, difficulties in determining the implantation site in the patient or to problems during the operation. The aim is therefore to determine from all the solutions adapted to all four grades, which are robust regarding the different dispersions; this is then described as the robustness of the solutions. We suggest making dispersions of the design variables in order to verify that the solutions that have been found remain solutions despite these dispersions. To do this, we set up a stochastic simulation around each of the solutions found. The imposed dispersions are shown in Table 5.

Table 5. Values of dispersion envisaged for each design variable.

	α_1 and α_2	K_{pr1} and K_{pr2}	BE_1 and BE_2
Dispersion	± 5°	± 100N.mm^{-1}	± 5mm

By introducing dispersions into the model developed above, it can be seen that the configurations become asymmetrical. Thus this indicates that the angle variation depends on the frontal direction, in contrast to the previous configurations.

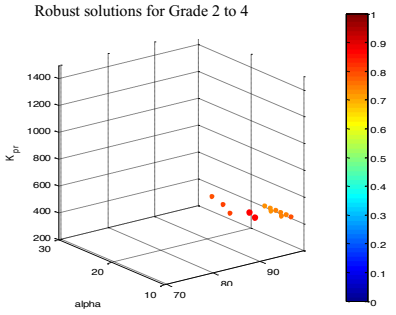

Fig. 8. Location of the robust solutions.

The dispersions lead to reduce the relevant solutions for the DSI. Figure 8 illustrates the location of solutions in the design space and it can be observed a drastic reduction of the amount of solutions (13 against 369 initial solutions drawn in Figure 7). They correspond to robust solutions and angular values close to 20°, lengths BE_i to 77mm and stiffness value for DSI to 360N.mm^{-1}. With this combination of the design variables, the DSI will remain a solution in spite of the dispersions listed in Table 5.

5. Conclusion

In this study, a design and an optimization of a dynamic spinal implant has been performed. To support the design optimization process it is proposed to use a general framework called OIA framework based on successive modeling: Observation, Interpretation and Aggregation. This approach is useful to integrate into the same structure the physical model, the design objectives and the requirements into one single objective to optimize (named GDI). A direct comparison of solutions is possible through the GDI value. On the first step, the design problem is optimized as a tradeoff between the grades of degeneration of the patient. Relevant solutions have been identified. From these solutions, robust evaluation of the solution has been performed since the surgical act leads to imprecision in angle and position of the DSI. In this context, it seems to be relevant to add robustness aspects into the search for a solution. Disparities on the design parameters (for angular values, the length BE and the stiffness values of DSI) have been included into the optimization process by using the previous developed framework.

This preliminary study will be completed through different axes. The first one consists in introducing the different natural motions of the vertebrae. This point will lead to completing the physical model of the OIA framework. To quantify the influence of the DSI on the final positions and motions of vertebrae, it is relevant to use the pseudo-rigid body model of the lumbar spine developed by [9]. These different points will lead to designing a robust and relevant DSI according to the different kinds of patients and recommendations could be deduced for required precision of the surgical act.

References

[1] Etebar S, Cahill DW. Risk factors for adjacent-segment failure following lumbar fixation with rigid instrumentation for degenerative instability. J of neurosurgery 1999;90(2):163-9.
[2] Kaner T, Sasani M, Oktenoglu T, Ozer AF. Dynamic stabilization of the spine: A New Classification System. Turk Neurosurg 2010;20(2):205-15.
[3] Molinari RW, Dahl J, Gruhn WL, Molinari WJ. Functional outcomes, morbidity, mortality, and fracture healing in 26 consecutive geriatric odontoid fracture patients treated with posterior fusion. J of Spinal Disorders and Techniques 2013;26(3):119-26.
[4] Barrey CY, Boissiere L, D'Acunzi G, Perrin G. One-stage combined lumbo-sacral fusion by anterior then posterior approach: Clinical and radiological results. European Spine J 2013;22(6):957-64.
[5] Monède-Hocquard L, Mesnard M, Ramos A, Gille O. Selection of polymer material in the design optimization of a new dynamic spinal implant. Advances in Biomechanics and Applications 2015;2(1):41-52.
[6] Rios-Zapata D, Duarte R, Nadeau JP, Pailhes J, Meija-Gutierrez R, Mesnard M. Patent-based creativity method for early design stages: case study in locking systems for medical applications. Int J on Interactive Design and Manufacturing 2016:1-13.
[7] Guérin P. Evaluation biomécanique in vitro du système de stabilisation dynamique B Dyn, influence sur la mobilité, la pression discale et les contraintes facettaires. Mémoire ENSAM Paris 2009.
[8] Shin DS, Lee K, Daniel Kim D. Biomechanical study of lumbar spine with dynamic stabilization device using finite element method. Computer-Aided Design 2007;39:559-67.
[9] Halverson PA, Bowden AE, Howell L. A pseudo-rigid-body model of the human spine to predict implant-induced changes on motion. J Mechanisms Robotics 2011;3(4):041008.
[10] Ledoux Y, Mesnard M, Peñaloza Sandoval JA, Perry N. Optimization of a dynamic intervertebral lumbar implant. Procedia CIRP 2016;50:192-7.
[11] Collignan A, Sebastian P, Pailhès J, Ledoux Y. Optimization of product in dynamic design space and selection through the arc-elasticity concept. Int J on Interactive Design and Manufacturing 2011;5(4):243-54.
[12] Quirante T, Sebastian P, Ledoux Y. A trade-off function to tackle robust design problems in engineering. J Engineering Design 2013;24(1):64-81.
[13] Quirante T, Ledoux Y, Sebastian P. Multiobjective optimization including design robustness objectives for the embodiment design of a two-stage flash evaporator. Int J on Interactive Design and Manufacturing 2012;6(1):29-39.
[14] Sebastian P, Ledoux Y, Collignan A, Pailhes J. Linking objective and subjective modeling in engineering design through arc-elastic dominance. Expert Systems and Applications 2012;39:7743-56.
[15] Harrington EC. The desirability function. Industrial Quality Control 1965;21(10):494-8.

.